Chemical Science

ROYAL SOCIETY OF CHEMISTRY

EDGE ARTICLE

View Article Online
View Journal

Check for updates

Cite this: DOI: 10.1039/d5sc08339g

All publication charges for this article have been paid for by the Royal Society of Chemistry

Nuclear quantum effects and vibrational resonances in organic hydrates: theoretical and experimental insights from DMSO monohydrate

Giacomo Botti[a] and Giacomo Mandelli*[b]

Received 28th October 2025
Accepted 10th February 2026

DOI: 10.1039/d5sc08339g

rsc.li/chemical-science

In the present work, we apply first-principles semiclassical dynamics to investigate a characteristic vibrational resonance in organic monohydrates, between the hydrogen-bonded OH stretching (OHb) and a three-quanta combination band composed of the water bending overtone coupled to a libration (b2lib). A reliable method to interpret and predict this feature would open the path to a new understanding of vibrational energy dissipation in aqueous media. Using the multiple-coherent semiclassical initial-value representation (MCSCIVR) with on-the-fly *ab initio* molecular dynamics, we compute vibrational densities of states that explicitly include zero-point energy, overtones, and combination bands without any *ad hoc* scaling procedures. Thanks to these exact quantum mechanical insights, we are able to directly observe and identify the b2lib combination band and thus the libration involved in the resonance effects. The computational procedure is further calibrated on available experimental data on acetone and cycloheptanone monohydrates. Then, it was applied to the newly obtained experimental spectrum for the dimethylsulfoxide monohydrate, provided by our collaborators Suhm and coworkers. Our results support the generality of the b2lib OHb intensity-borrowing mechanism across monohydrates and underscore the power of MCSCIVR to resolve nuclear-quantum effects in hydrated systems.

Experimental vibrational spectroscopy records all the allowed transitions between the vibrational quantum states of the molecules under examination. The main transitions are called fundamentals and occur between the ground state and the first excited states of each vibrational chromophore. In addition, experimental spectra can detect transitions involving states that rest at a higher energy than the corresponding fundamental.

These transitions are classified either as overtones or combination bands. A quantum overtone is a single-mode excitation toward a state with energy higher than the fundamental one. Similarly, a quantum combination band represents a transition to a higher energy state thanks to more than one-mode excitation. Both of these vibrational features are multi-state, single-photon excitations. Usually, they are not very intense, since they are prohibited (in double-harmonic approximation) by the selection rules. However, it is possible for an overtone or a combination to "steal" intensity from a neighboring allowed transition *via* a resonance interaction. The resonance allows the mixing of vibrational states of similar energy and symmetry, resulting in the less intense transition borrowing intensity from the more intense one. The most common borrowing is occurring between two fundamentals, and it is called Fermi resonance.[1–6]

This resonance is the footprint of a strong coupling between the involved states. This coupling is described, from a classical point of view, as mechanical coupling and represents a redistribution pathway for the total vibrational energy. Typically, strongly coupled vibrational modes involve the same set of atoms. When a resonance occurs between inter- and intramolecular vibrational modes, the coupling opens an efficient pathway for rapid vibrational energy dissipation.[7] Notably, when one of the interacting species is a prototypical solvent such as water, this effect yields valuable insights into the nature of molecular hydration.

In this regard, Suhm and coworkers highlighted the role of these types of couplings in the vibrational resonances occurring in carbonyl monohydrates, providing state-of-the-art experimental spectra.[8] All these resonances involve the H-bonded OH stretching (OHb) and the combination band between a specific water libration and the first overtone of the water bending (referred to as b2lib), see Fig. 1. As observed experimentally, the fingerprint of the borrowing is the intensity loss of the OHb stretching fundamental and the appearance of the combination band in the spectrum, which may exhibit lower or higher frequency than the OHb stretching peak. This resonance

---

[a] University of South Carolina, Department of Chemistry and Biochemistry, 631 Sumter St, Columbia, SC 29208, USA

[b] Politecnico di Milano, Department of Chemistry, Materials, and Chemical Engineering "Giulio Natta", Piazza Leonardo da Vinci 32, 20133 Milan, Italy. E-mail: giacomo.mandelli@polimi.it

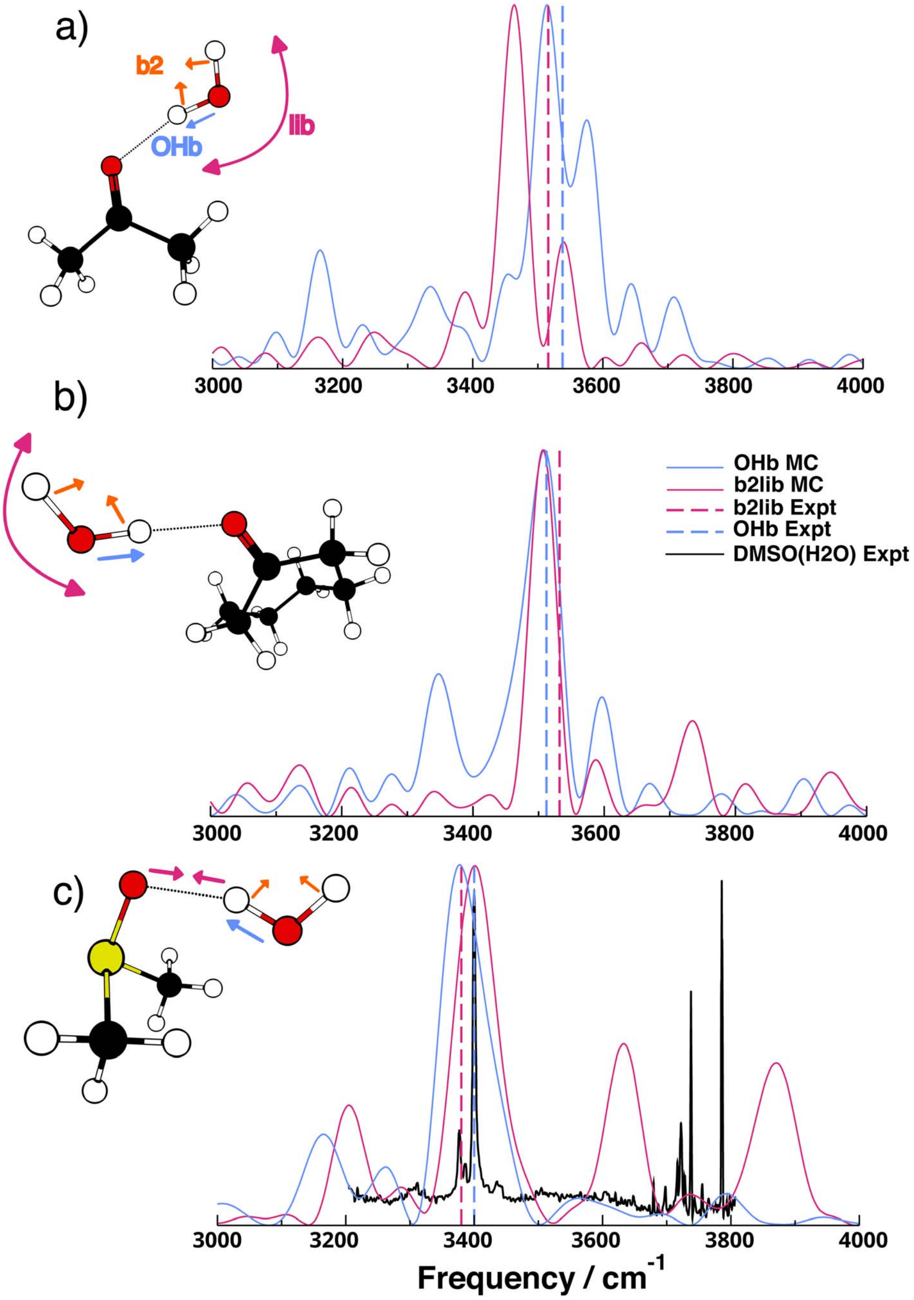

Fig. 1 Vibrational spectra studied in the present paper with the computed and the experimental spectra involving the resonance between the combination band of the bending overtone and libration motion bnd_2 + lib (b2lib) and the hydrogen-bonded OHb stretching. Panel (a): semiclassical vibrational spectra for the acetone monohydrate (Ace·H_2O). A Pictorial representation of the prototypical acetone monohydrate normal modes involved in the resonant interaction is also provided. Panel (b): semiclassical vibrational spectra for the cycloheptanone monohydrate (Cen·H_2O). Panel (c): semiclassical and experimental vibrational spectra for the dimethylsulfoxide monohydrate (DMSO·H_2O).

involving a fundamental state and a three-quanta combination band is classified as a (1,3) Darling–Dennison resonance, following Rosnik *et al.* classification.[9–11] This spectral feature was registered in a variety of carbonyl monohydrate spectra and was interpreted using scaled harmonic frequencies and a simplified VPT2+K model by Suhm *et al.*[8] With this initial analysis and the experimental evidence, they concluded that such resonance should happen in a more or less pronounced form, whenever the OHb stretching transition falls to around 3500 cm^{-1}, close to the b2lib estimated energy.

In the present work, we show that this feature should be common to all monohydrate compounds meeting the energetic and mechanical requirements, and not only in carbonyl monohydrates. This hypothesis suggests a critical energy pathway for vibrational relaxation between the high-energy, intermolecular OHb stretching mode and the low-energy, intramolecular librations, facilitated by the water bending mode.[7,12–15]

To this day, vibrational theories applicable to a molecular system (such as harmonic approximation or VPT2+K) lack an organic treatment of overtones and combination bands, since they usually predict them as weighted sums of the fundamental transitions and not as quantum states *per se*.[10] Moreover, these methods were found lacking in describing the potential anharmonicity, even in fundamental transitions, when compared with dynamical methods. This was evident in a recent vibrational spectroscopy blind challenge focused on organic molecule monohydrates.[16] In addition to that, in real systems, there are quantum overtones and combination bands,[17] which are nuclear quantum effects that cannot be described rigorously even when using state-of-the-art classical simulations, such as quasiclassical trajectory (QCT) methods.[16,18–20]

For these reasons, we decided to employ semiclassical dynamics to obtain the vibrational spectra of acetone monohydrate (Ace$\cdot$H$_2$O), cycloheptanone monohydrate (Cen$\cdot$H$_2$O), and dimethylsulfoxide monohydrate (DMSO$\cdot$H$_2$O). Semiclassical dynamics is a well-established method of including quantum effects into inexpensive classical dynamics.[20–22] In particular, the versatility of the multiple coherent semiclassical initial value representation (MCSCIVR) approach made possible the study of the vibrational spectra of small biomolecules,[23–28] supramolecular complexes of biological interest,[29,30] and molecules embedded in a solvent box or adsorbed on surfaces.[31–33]

MCSCIVR uses a single tailored classical trajectory and the instantaneous Hessian to collect a vibrational spectrum that includes quantum effects such as zero point energies, overtones and tunneling splittings.[20,23,26,34–36] This allowed us to recover the quantum vibrational density of states (VDOS) and pinpoint the combination band location as a quantum state and without any assumptions, scaling, or other *ad hoc* parameters, and with a manageable computational effort. This approach proved to be a sound framework to rigorously investigate the H bond effects involved in the peculiar b2lib resonance and to test the hypothesis of its universality, proposed by Suhm and coworkers.[8,37,38]

At the core of MCSCIVR, there is the ability to recover the accurate estimate of vibrational eigenvalues and eigenfunctions from a single classical trajectory, provided the trajectory energy is reasonably close to the true eigenvalue.[39] Indeed, the simulation is launched near the true quantum mechanical values using quantized harmonic conditions

$$\begin{cases} p_i(0) & = \sqrt{\hbar\omega_i(2n_i+1)} \\ q_i(0) & = q_i^{(\mathrm{eq})} \end{cases}. \tag{1}$$

where the initial momentum in mass-scaled coordinates for the normal mode i is proportional to the square root of the relative harmonic frequency ω_i and the vibrational quantum number n_i. The initial position is chosen to match the equilibrium geometry. By adding quanta of excitation to a normal mode, one can enhance the mode prominence, leading to a more accurate estimate of that mode's frequency. The final formulation for the MCSCIVR power spectrum is the following[40–43]

$$I(E) = \left(\frac{1}{2\pi\hbar}\right)^{N_\mathrm{v}} \iint \mathrm{d}\mathbf{p}_0\mathrm{d}\mathbf{q}_0 \frac{1}{2\pi\hbar T}$$

$$\left| \int_0^T \mathrm{d}t e^{\frac{i}{\hbar}[S_t(\mathbf{p}_t,\mathbf{q}_t)+Et+\phi_t(\mathbf{p}_t,\mathbf{q}_t)]} \langle\chi|g_t(\mathbf{p}_t,\mathbf{q}_t)\rangle \right|^2, \tag{2}$$

where E is the absolute vibrational energy, N_v is the dimension of the vibrational space, ($\mathbf{p}_0$, $\mathbf{q}_0$) are the initial conditions, T is the total length of the trajectory, $S_t(\mathbf{p}_t, \mathbf{q}_t)$ is the instantaneous classical action, $\phi_t(\mathbf{p}_t, \mathbf{q}_t)$ the prefactor phase, and $\langle\chi|g_t(\mathbf{p}_t, \mathbf{q}_t)\rangle$ is the quantum overlap between an arbitrary reference state $|\chi\rangle$ and a coherent state evolved for a time t ($|g_t\rangle$). Coherent states have a Gaussian spatial representation with a width defined by harmonic frequencies of vibration. The evolution of the prefactor phase $\phi_t(\mathbf{p}_t, \mathbf{q}_t)$ requires the Hessian matrix at each step of the trajectory integration. To improve the sampling while using a single trajectory, the MCSCIVR reference state is built using two coherent states per normal mode[34,36]

$$|\chi\rangle = \prod_j^{N_\mathrm{v}} \left\{ \left|\mathbf{p}_{\mathrm{eq},j}, \mathbf{q}_{\mathrm{eq},j}\right\rangle + \varepsilon_j \left| -\mathbf{p}_{\mathrm{eq},j}, \mathbf{q}_{\mathrm{eq},j}\right\rangle \right\} \tag{3}$$

where ($\mathbf{p}_{\mathrm{eq},j}$, $\mathbf{q}_{\mathrm{eq},j}$) are the equilibrium coordinates and momenta of the j-th vibrational mode. By changing the value of the weight ε_j, one can collect the spectrum of the zero-point energy ($\varepsilon_j = 1$, $\forall j$) or of the j-th normal mode ($\varepsilon_j = -1$). It is also possible to build the braket using harmonic states. In this case, the reference state $|\chi\rangle$ is the product of the Harmonic Oscillator (HO) eigenstates that represent the desired state of the system. In this way, the ZPE is obtained by using the ground eigenstate in all normal modes, whereas the signal for a certain mode fundamental is selected by using the first excited HO eigenstate for that mode. The harmonic reference state is particularly useful when searching for signals of overtones and combination bands, as it filters the signal based on the state composition rather than the symmetry of the states, making the identification of these elusive features more straightforward. For these reasons, the harmonic reference state was initially employed to build the semiclassical vibrational wavefunctions, which can be employed to compute the semiclassical IR spectrum.[25,26,44,45] The reference state is arbitrary, so there is no difference in the energy values obtained using the coherent or the harmonic reference state. Taking into account the limitations of MCSCIVR—such as the limited sampling time, and the single-trajectory approach—we expect some uncertainty in the treatment of librational modes. Nonetheless, these are well-known limitations, and MCSCIVR remains a reliable and effective approach for vibrational spectroscopy, particularly for identifying nuclear quantum features. Further theoretical details on MCSCIVR can be found in the SI.

To assess the accuracy of the simulation setup, preliminary calculations were done using B3LYP-D3BJ/def2-TZVPD level of theory on Ace$\cdot$H$_2$O and Cen$\cdot$H$_2$O, for which previous experimental results were available. The simulation results are compared against the bound water vibrational frequencies in Table 1. The mean absolute error (16 cm) for both systems gives

Table 1 Harmonic (Harm), MCSCIVR (SC), and experimental (Expt) frequencies in cm^{-1} for $ACE\cdot H_2O$ and $CEN\cdot H_2O$. The mean absolute error (MAE) for the harmonic and MCSCIVR results with respect to the experimental frequencies is included

	$Ace\cdot H_2O$				$Cen\cdot H_2O$			
Mode	State	Harm	MCSCIVR	Expt	State	Harm	MCSCIVR	Expt
OH str	33_1	3855	3731	3723	63_1	3854	3750	3721
OHb str	32_1	3599	3514	3538	62_1	3576	3509	3512
MAE	—	96	16	—	—	98	16	—
b2lib	$8_1 24_2$	3701	3464	3516	$11_1 48_2$	3716	3507	3532

us an indicative accuracy estimate for our simulation, in line with other SCIVR investigations.[27,28,30,46]

Thereafter, we verified the presence and the positions of the combination bands. To identify the libration involved in the combination band, we started from the assignment provided by Suhm *et al.*, looking for a mode around 300 cm.[8] We employed the normal mode analysis at the equilibrium geometry to choose the most suitable vibrations. As customary in vibrational analysis, we classified the normal modes by ordering them with increasing energy. The corresponding vibrational state is indicated as m_n, where m is the normal mode number and n is the number of quanta in the vibrational state. Since this was proposed as a universal resonance, we focused on the libration modes, which imply similar molecular displacements in the two systems. To improve the description of the b2lib combination band, a quantum of excitation was provided to the bending mode of water (therefore $n_{\text{bnd}} = 1$). Computational details about the parameters for the on-the-fly molecular dynamics can be found in the SI. The combination band VDOS signal was filtered by selecting the harmonic reference state corresponding to the possible b2lib final state (first excited eigenstate for the libration under investigation, second excited eigenstate for the water bending). In this way, the spectrum of each b2lib combination band can be compared with that of the OHb stretching, selecting as resonance partner the closest in energy. The spectra of the examined b2lib combination bands are reported in the SI.

Starting from the $Ace\cdot H_2O$ system, the spectrum is shown in Fig. 1 panel a. The most likely resonant partners are the OHb hydrogen bonded stretching mode (32_1) and the b2lib combination ($8_1 24_2$) between the bending overtone (24_2) and the libration (8_1). The 8_1 libration mode is a water frustrated rotation coplanar with the C=O bond. Some early data of the $Ace\cdot H_2O$ investigation have been reported in ref. 33. For the $Cen\cdot H_2O$, the resonance is most likely between the OHb mode (62_1) and the $11_1 48_2$ b2lib combination band, see Fig. 1 panel b. The 11_1 libration is similar to the 8_1 of the $Ace\cdot H_2O$ system, being the water frustrated rotation coplanar with the carbonyl bond.

Remarkably, as we can see from the relative positions of the MCSCIVR peaks, the nuclear quantum effects involved in the b2lib and the resonant interaction with the hydrogen-bonded stretching are accurately reproduced and accounted for. The main difference between the two examined systems is the position of the OHb signal, which follows the b2lib peak in the $Ace\cdot H_2O$ spectrum, but precedes the same in the $Cen\cdot H_2O$ one. Our setup can reliably identify the resonant combination band, but we have to account for its inherent error mainly due to the *ab initio* method limitations. For this specific case, we estimated this error using the OH stretching MAE reported in Table 1, and found it very close ($16\ cm^{-1}$) to the experimental resonance splitting of $15\ cm^{-1}$. Given the recognized MCSCIVR accuracy, the method is more accurate than either the scaled harmonic previously employed or the VPT2+K treatment included in the SI from Fischer *et al.* paper.[8] In addition, the attribution is not predicated on the faithful reproduction of the spectral features, but on the harmonic reference state filter and the MCSCIVR energy matching: the former selects faithfully the desired vibrational state contribution to the VDOS, the latter allows to check that the energetic resonance condition is met. In this way, we proceeded not by relying on the method's higher accuracy, but by resolving the signals of the b2lib candidates and selecting the one closest in energy to the OHb state with the compatible mechanical requirements.

We decided to investigate further whether this spectral quantum feature can be reliably captured in other monohydrate complexes, as hypothesized in the literature.[8,12] This will be the first step in understanding the universality of this quantum resonance and its importance in quantum vibrational energy dissipation pathways. Therefore, we chose the dimethylsulfoxide (DMSO) water complex because of its peculiar H bond, presenting a higher H-bond strength and a different water orientation, with respect to the other dimers, as shown in Fig. 1 panel c. Indeed, water rests on the DMSO mirror plane, whereas the water molecule of the other dimers is coplanar with the carbonyl bond, attacking the carbonyl moiety at an angle. In addition to that, the strength of $DMSO\cdot H_2O$ H bond pushes the OHb frequency much lower than any carbonyl compound, changing the energy required to participate in the resonance. Finally, the DMSO-water mixture is widely used as a cryoprotectant in biological applications,[47] due to its unusually low freezing eutectic point, which is not yet fully understood.[48–53] For this reason, any advance in the understanding of the water-DMSO interaction could be essential for unraveling this elusive behaviour.

The new DMSO monohydrate experimental vibrational spectrum was obtained by M. Boedecker and T. Fischer, who courteously made it available for us. The full spectrum is available in the Göttigen Research Online Data repository,[54] while the portion of our interest is included in the SI. The spectrum is obtained using a cutting-edge slit jet FTIR spectrometer, described by Suhm and coworkers in ref. 55.

The experimental spectrum (Fig. 1 panel c) presents the expected resonance feature for the hydrogen-bonded OH stretching. From our semiclassical analysis, performed with the same setup as those of Ace$\cdot$$H_2O$ and Cen$\cdot$$H_2O$, the only combination band compatible for the DMSO$\cdot$$H_2O$ b2lib is the $5_1 25_2$ at 3400 cm^{-1}, which partially overlaps with the OHb mode at 3380 cm^{-1} (Table 2). The starting geometry for the DMSO$\cdot$$H_2O$ simulation was selected by conformational analysis using Crest.[56] The results are reported in SI. The inversion of the peaks position with respect to the experiment prompted us to further validate our results by running an additional simulation with the ωB97X functional. The results confirm our assignment, even though ωB97X both harmonic and MCSCIVR frequencies are less accurate than the B3LYP ones. The results are reported in the SI. Although the MCSCIVR approach yields highly accurate vibrational frequencies, remaining inaccuracies in the potential energy surface (PES) still influence the predicted spectral features, leading to more noticeable discrepancies, as we can see by comparing the harmonic and MCSCIVR estimates obtained with B3LYP and ωB97X functionals. In MCSCIVR analyses, it is customary to compare only peak maxima, so the two simulated transitions appear "inverted". However, by looking at the peak shape, it is more appropriate to describe them as overlapping. In this context, such overlap is an acceptable outcome, since the computed signals lie only 20 cm^{-1} from the experimental band—an agreement that is better than what alternative methods typically achieve (see Tables S1 and S2). This accuracy is compatible with the results from the literature.[27,28,30,46] Taking into account that MCSCIVR could not reach the experiment resolution, the assignment was conducted by first computing all the possible b2lib modes, then by selecting the ones involving the water molecule, and finally by selecting the one matching in energy with the simulated OHb signal. For the discarded spectra, see Fig. S6 and S7.

The 5_1 libration motion is an accordion motion involving both DMSO and water, as opposed to the pure water frustrated rotation of Ace$\cdot$$H_2O$ 8_1 and Cen$\cdot$$H_2O$ 11_1. For this reason, the b2lib resonant mode in DMSO$\cdot$$H_2O$ should be more properly labeled as b2OO, in analogy with the nomenclature used by Suhm *et al.* for combination of monohydrate amines (b2ON).[38] This new experiment supports the idea that "universality" of this resonance extends beyond the carbonyl monohydrates. However, our vibrational analysis concludes that even if the same resonance appears, the resonant combination band is not the same: both the mechanical and energetic requirements must be met. Indeed, the resonance should appear only when the transition energies match and when a mechanical coupling opens the way for an energy transfer. In other words, the b2lib closest to the OHb will be the one that enters into resonance, and the libration-bending coupling will ensure that the mechanical requirements are met, at least in these types of complexes. The change of the involved libration is not reflected in the vibrational spectrum and can only be captured by the vibrational state selectivity afforded by the MCSCIVR formulation. We must point out that assigning the right libration inside the resonance is not trivial at all for spectral assignment purposes, and it can have a substantial impact on the vibrational energy redistribution pathways available to the system, and in the study of DMSO and H_2O interaction in general.

Table 2 Harmonic (Harm), MCSCIVR (SC), and experimental (Expt) frequencies in cm^{-1} for DMSO$\cdot$$H_2O$ and CEN$\cdot$$H_2O$. The mean absolute error (MAE) for the harmonic and MCSCIVR results with respect to the experimental frequency is included

	DMSO$\cdot$$H_2O$			
Mode	State	Harm	MCSCIVR	Expt
OH str	33_1	3854	3750	3718
OHb str	32_1	3480	3380	3400
MAE	—	108	26	—
b2lib	$5_1 25_2$	3510	3400	3380

To summarize, in this work we applied semiclassical dynamics to investigate an intrinsically quantum feature of the vibrational spectra of monohydrate complexes. Using MCSCIVR ability to filter the signal relative to a single vibrational state,[25] we identified the b2lib combination band responsible for the resonance reported by Fischer *et al.*[8] Using MCSCIVR, which intrinsically includes nuclear quantum effects and anharmonicities, the combination bands come out naturally in the power spectrum, and no assumption needs to be made, even when the combination occurs with an overtone as in these cases.[20] Both in Ace$\cdot$$H_2O$ and Cen$\cdot$$H_2O$ complexes, the libration involved is a frustrated rotation of water in the same plane of the carbonyl bond. By expanding this analysis to the DMSO$\cdot$$H_2O$ complex, we discovered that—even if the resonance is still present—the involved libration is now changed, due to the different OHb energy and complex geometry. This is a crucial information not only for extending the investigation beyond carbonyl compounds, but also for gathering insights on the accessible pathways for vibrational energy redistribution in water-solvated systems. Thus, we showed how one can use state-of-the-art experimental vibrational spectroscopy in concert with quantum simulation methods to collect and rationalize data that could have a significant impact on related investigations.

Author contributions

Giacomo Botti: software, methodology, conceptualization, review, editing, writing – original draft. Giacomo Mandelli: software, methodology, conceptualization (lead), review, editing, writing – original draft (lead).

Conflicts of interest

There are no conflicts to declare.

Data availability

The data that support the findings of this study are available from the corresponding author upon reasonable request.

Supplementary information (SI): (1) brief overview of the theoretical background; (2) DMSO conformational and normal mode analysis; (3) vibrational spectra; (4) molecular dynamics and parameters; (5) optimized geometries. See DOI: https://doi.org/10.1039/d5sc08339g.

Acknowledgements

This material is based upon work supported in part by the National Science Foundation of U.S.A. under Grant No. CHE-2308922. The authors thank Professor Martin Suhm (University of Göttingen) and his research group for providing the experimental data and for the insightful suggestions on the manuscript. The authors gratefully acknowledge Professor Nino Famulari (Politecnico di Milano) and Sophya Garashchuk (University of South Carolina) for their suggestions and the support provided during the authors' time in their research group. Finally, the authors thanks Michele Ceotto (Università degli Studi di Milano) for his guidance, and finally for prompting us to write this paper.

References

1 D. C. Harris and M. D. Bertolucci, *Symmetry and Spectroscopy: An Introduction to Vibrational and Electronic Spectroscopy*, Dover Publications, New York, 1989.

2 J. A. Stride, P. H. Dallin and U. A. Jayasooriya, Intermolecular fermi resonance, *J. Chem. Phys.*, 2003, **119**, 2747–2752.

3 F. Kollipost, A. V. Domanskaya and M. A. Suhm, Microscopic roots of alcohol–ketone demixing: infrared spectroscopy of methanol–acetone clusters, *J. Phys. Chem.*, 2015, **119**, 2225–2232.

4 N. Mao, S. Huang, L. G. Pimenta Martins, H. Yan, X. Ling, L. Liang, J. Kong and W. A. Tisdale, Vibrational Fermi Resonance in Atomically Thin Black Phosphorus, *Nano Lett.*, 2024, **24**, 12582–12589.

5 S. Zhang, W. Fang, B. Zhao, W. Zhang and Z. Men, Pressure-induced hydrogen bonding modulating Fermi resonance between fundamental modes in xylitol molecule, *Spectrochim. Acta, Part A*, 2024, **320**, 124641.

6 Q.-R. Huang, T. Endo, S. Mishra, B. Zhang, L.-W. Chen, A. Fujii, L. Jiang, G. N. Patwari, Y. Matsuda and J.-L. Kuo, Understanding Fermi resonances in the complex vibrational spectra of the methyl groups in methylamines, *Phys. Chem. Chem. Phys.*, 2021, **23**, 3739–3747.

7 D. J. Nesbitt and R. W. Field, Vibrational Energy Flow in Highly Excited Molecules: Role of Intramolecular Vibrational Redistribution, *J. Chem. Phys.*, 1996, **100**, 12735–12756.

8 T. L. Fischer, T. Wagner, H. C. Gottschalk, A. Nejad and M. A. Suhm, A Rather Universal Vibrational Resonance in 1:1 Hydrates of Carbonyl Compounds, *J. Phys. Chem. Lett.*, 2021, **12**, 138–144.

9 B. T. Darling and D. M. Dennison, The Water Vapor Molecule, *Phys. Rev.*, 1940, **57**, 128–139.

10 A. M. Rosnik and W. F. Polik, VPT2+K Spectroscopic Constants and Matrix Elements of the Transformed Vibrational Hamiltonian of a Polyatomic Molecule with Resonances Using Van Vleck Perturbation Theory, *Mol. Phys.*, 2014, **112**, 261–300.

11 G. Mandelli, C. Aieta and M. Ceotto, Heavy Atom Tunneling in Organic Reactions at Coupled Cluster Potential Accuracy with a Parallel Implementation of Anharmonic Constant Calculations and Semiclassical Transition State Theory, *J. Chem. Theory Comput.*, 2022, **18**, 623–637.

12 P. R. Rablen, J. W. Lockman and W. L. Jorgensen, Ab Initio Study of Hydrogen-Bonded Complexes of Small Organic Molecules with Water, *J. Phys. Chem. A*, 1998, **102**, 3782–3797.

13 K. E. Otto, Z. Xue, P. Zielke and M. A. Suhm, The Raman Spectrum of Isolated Water Clusters, *Phys. Chem. Chem. Phys.*, 2014, **16**, 9849.

14 K. Schwing, C. Reyheller, A. Schaly, S. Kubik and M. Gerhards, Structural Analysis of an Isolated Cyclic Tetrapeptide and Its Monohydrate by Combined IR/UV Spectroscopy, *ChemPhysChem*, 2011, **12**, 1981–1988.

15 E. G. Robertson, M. R. Hockridge, P. D. Jelfs and J. P. Simons, IR-UV Ion-Dip Spectroscopy of *N*-Benzylformamide Clusters: Stepwise Hydration of a Model Peptide, *J. Phys. Chem. A*, 2000, **104**, 11714–11724.

16 T. L. Fischer, M. Bödecker, S. M. Schweer, J. Dupont, V. Lepère, A. Zehnacker-Rentien, M. A. Suhm, B. Schröder, T. Henkes, D. M. Andrada, *et al.*, The First HyDRA Challenge for Computational Vibrational Spectroscopy, *Phys. Chem. Chem. Phys.*, 2023, **25**, 22089–22102.

17 G. Botti, Classical Combination Frequencies in Vibrational Spectra, *J. Chem. Phys.*, 2025, **163**, 214116.

18 M. L. Koszykowski, D. W. Noid and R. A. Marcus, Semiclassical Theory of Intensities of Vibrational Fundamentals, Overtones, and Combination Bands, *J. Phys. Chem.*, 1982, **86**, 2113–2117.

19 A. Rognoni, R. Conte and M. Ceotto, Caldeira–Leggett Model *vs. Ab Initio* Potential: A Vibrational Spectroscopy Test of Water Solvation, *J. Chem. Phys.*, 2021, **154**, 094106.

20 R. Conte, C. Aieta, G. Botti, M. Cazzaniga, M. Gandolfi, C. Lanzi, G. Mandelli, D. Moscato and M. Ceotto, Anharmonicity and Quantum Nuclear Effects in Theoretical Vibrational Spectroscopy: A Molecular Tale of Two Cities, *Theor. Chem. Acc.*, 2023, **142**, 53.

21 S. Malpathak, M. S. Church and N. Ananth, A Semiclassical Framework for Mixed Quantum Classical Dynamics, *J. Phys. Chem. A*, 2022, **126**, 6359–6375.

22 J. Vanicek, Family of Gaussian Wavepacket Dynamics Methods from the Perspective of a Nonlinear Schrödinger Equation, *J. Chem. Phys.*, 2023, **159**, 014114.

23 R. Conte, A. Aspuru-Guzik and M. Ceotto, Reproducing Deep Tunneling Splittings, Resonances, and Quantum Frequencies in Vibrational Spectra From a Handful of Direct Ab Initio Semiclassical Trajectories, *J. Phys. Chem. Lett.*, 2013, **4**, 3407–3412.

24 F. Gabas, R. Conte and M. Ceotto, On-the-Fly Ab Initio Semiclassical Calculation of Glycine Vibrational Spectrum, *J. Chem. Theory Comput.*, 2017, **13**, 2378–2388.

25 C. Aieta, G. Bertaina, M. Micciarelli and M. Ceotto, Representing Molecular Ground and Excited Vibrational Eigenstates with Nuclear Densities Obtained from

Semiclassical Initial Value Representation Molecular Dynamics, *J. Chem. Phys.*, 2020, **153**, 214117.

26 C. Aieta, M. Micciarelli, G. Bertaina and M. Ceotto, Anharmonic Quantum Nuclear Densities from Full Dimensional Vibrational Eigenfunctions with Application to Protonated Glycine, *Nat. Commun.*, 2020, **11**, 4348.

27 G. Botti, M. Ceotto and R. Conte, On-the-Fly Adiabatically Switched Semiclassical Initial Value Representation Molecular Dynamics for Vibrational Spectroscopy of Biomolecules, *J. Chem. Phys.*, 2021, **155**, 234102.

28 G. Botti, C. Aieta and R. Conte, The Complex Vibrational Spectrum of Proline Explained through the Adiabatically Switched Semiclassical Initial Value Representation, *J. Chem. Phys.*, 2022, **156**, 164303.

29 F. Gabas, R. Conte and M. Ceotto, Semiclassical Vibrational Spectroscopy of Biological Molecules Using Force Fields, *J. Chem. Theory Comput.*, 2020, **16**, 3476–3485.

30 G. Botti, M. Ceotto and R. Conte, Investigating the spectroscopy of the gas phase guanine–cytosine pair: Keto versus enol configurations, *J. Phys. Chem. Lett.*, 2023, **14**, 8940–8947.

31 D. Moscato, F. Gabas, R. Conte and M. Ceotto, Vibrational Spectroscopy Simulation of Solvation Effects on a G-quadruplex, *J. Biomol. Struct. Dyn.*, 2023, 1–11.

32 M. Cazzaniga, M. Micciarelli, F. Moriggi, A. Mahmoud, F. Gabas and M. Ceotto, Anharmonic Calculations of Vibrational Spectra for Molecular Adsorbates: A Divide-and-Conquer Semiclassical Molecular Dynamics Approach, *J. Chem. Phys.*, 2020, **152**, 104104.

33 R. Conte, C. Aieta, M. Cazzaniga and M. Ceotto, A Perspective on the Investigation of Spectroscopy and Kinetics of Complex Molecular Systems with Semiclassical Approaches, *J. Phys. Chem. Lett.*, 2024, **15**, 7566–7576.

34 M. Ceotto, S. Atahan, G. F. Tantardini and A. Aspuru-Guzik, Multiple Coherent States for First-Principles Semiclassical Initial Value Representation Molecular Dynamics, *J. Chem. Phys.*, 2009, **130**, 234113.

35 M. Ceotto, S. Valleau, T. Gian Franco and A. Aspuru-Guzik, First Principles Semiclassical Calculations of Vibrational Eigenfunctions, *J. Chem. Phys.*, 2011, **134**, 234103.

36 M. Ceotto, S. Atahan, S. Shim, G. F. Tantardini and A. Aspuru-Guzik, First-Principles Semiclassical Initial Value Representation Molecular Dynamics, *Phys. Chem. Chem. Phys.*, 2009, **11**, 3861.

37 T. L. Fischer, C. V. Jensen, E. Lwin, D. Pal, H. G. Kjaergaard and M. A. Suhm, OH-stretching dynamics in trimethylamine monohydrate: what can we learn from three different direct absorption spectra?, *Phys. Chem. Chem. Phys.*, 2025, **27**, 11487–11491.

38 E. Lwin, N. O. Lüttschwager and M. A. Suhm, The universal vibrational dynamics of water bound to tertiary amines: more than just Fermi resonance, *Phys. Chem. Chem. Phys.*, 2025, **27**, 5808–5820.

39 N. De Leon and E. J. Heller, Semiclassical Quantization and Extraction of Eigenfunctions Using Arbitrary Trajectories, *J. Chem. Phys.*, 1983, **78**, 4005–4017.

40 W. H. Miller, Semiclassical Theory of Atom–Diatom Collisions: Path Integrals and the Classical S Matrix, *J. Chem. Phys.*, 1970, **53**, 1949–1959.

41 Y. Elran and K. G. Kay, Improving the Efficiency of the Herman–Kluk Propagator by Time Integration, *J. Chem. Phys.*, 1999, **110**, 3653–3659.

42 Y. Elran and K. G. Kay, Time-Integrated Form of the Semiclassical Initial Value Method, *J. Chem. Phys.*, 1999, **110**, 8912–8918.

43 A. L. Kaledin and W. H. Miller, Time Averaging the Semiclassical Initial Value Representation for the Calculation of Vibrational Energy Levels. II. Application to H2CO, NH3, CH4, CH2D2, *J. Chem. Phys.*, 2003, **119**, 3078–3084.

44 M. Micciarelli, R. Conte, J. Suarez and M. Ceotto, Anharmonic Vibrational Eigenfunctions and Infrared Spectra from Semiclassical Molecular Dynamics, *J. Chem. Phys.*, 2018, **149**, 064115.

45 M. Micciarelli, F. Gabas, R. Conte and M. Ceotto, An Effective Semiclassical Approach to IR Spectroscopy, *J. Chem. Phys.*, 2019, **150**, 184113.

46 R. Conte, G. Botti and M. Ceotto, Sensitivity of Semiclassical Vibrational Spectroscopy to Potential Energy Surface Accuracy: A Test on Formaldehyde, *Vib. Spectrosc.*, 2020, **106**, 103015.

47 K. A. Murray and M. I. Gibson, Chemical approaches to cryopreservation, *Nat. Rev. Chem.*, 2022, **6**, 579–593.

48 B. Kirchner and J. Hutter, The Structure of a DMSO–Water Mixture from Car–Parrinello Simulations, *Chem. Phys. Lett.*, 2002, **364**, 497–502.

49 B. Kirchner and M. Reiher, The Secret of Dimethyl Sulfoxide-Water Mixtures. A Quantum Chemical Study of 1DMSO- *n* Water Clusters, *J. Am. Chem. Soc.*, 2002, **124**, 6206–6215.

50 M. Reiher and B. Kirchner, A Wavefunction-Based Criterion for the Detection of Intermolecular Interactions in Molecular Dynamics Simulations, *J. Phys. Chem. A*, 2003, **107**, 4141–4146.

51 S. S. Stachura, C. J. Malajczuk and R. L. Mancera, Molecular Dynamics Simulations of a DMSO/Water Mixture Using the AMBER Force Field, *J. Mol. Model.*, 2018, **24**, 174.

52 A. Luzar and D. Chandler, Structure and Hydrogen Bond Dynamics of Water–Dimethyl Sulfoxide Mixtures by Computer Simulations, *J. Chem. Phys.*, 1993, **98**, 204107.

53 E. Lee and C. R. Baiz, How Cryoprotectants Work: Hydrogen-Bonding in Low-Temperature Vitrified Solutions, *Chem. Sci.*, 2022, **13**, 9980–9984.

54 T. L. Fischer, M. Bödecker and M. A. Suhm, *FTIR Jet Spectra DMSO + H2O*, 2025, DOI: 10.25625/TBDW5R.

55 H. C. Gottschalk, T. L. Fischer, V. Meyer, R. Hildebrandt, U. Schmitt and M. A. Suhm, A sustainable slit jet FTIR spectrometer for hydrate complexes and beyond, *Instruments*, 2021, **5**, 12.

56 P. Pracht, S. Grimme, C. Bannwarth, F. Bohle, S. Ehlert, G. Feldmann, J. Gorges, M. Müller, T. Neudecker, C. Plett, *et al.*, CREST—A Program for the Exploration of Low-Energy Molecular Chemical Space, *J. Chem. Phys.*, 2024, **160**, 114110.